

UC San Diego

UC San Diego Previously Published Works

Title

Peripheral-coupled-waveguide MQW electroabsorption modulator for near transparency and high spurious free dynamic range RF fiber-optic link

Permalink

<https://escholarship.org/uc/item/67j7r500>

Journal

IEEE Photonics Technology Letters, 16(9)

ISSN

1041-1135

Authors

Zhuang, Y L
Chang, WSC
Yu, PKL

Publication Date

2004-09-01

Peer reviewed

Peripheral-Coupled-Waveguide MQW Electroabsorption Modulator for Near Transparency and High Spurious Free Dynamic Range RF Fiber-Optic Link

Yuling Zhuang, William S. C. Chang, and Paul K. L. Yu

Abstract—Peripheral coupled waveguide (PCW) design has been deployed in InGaAsP multiple quantum-well (MQW) electroabsorption modulator (EAM) at 1.55- μm wavelength. PCW enhances the optical saturation power and reduces the optical insertion loss and the equivalent V_{π} simultaneously. A radio-frequency link using a 1.3-mm-long lumped-element PCW EAM has achieved experimentally a link gain of -3 dB, at 500 MHz and at input optical power of 80 mW. The corresponding two-tone multioctave spurious-free dynamic range (SFDR) at the same bias is measured at $118 \text{ dB} \cdot \text{Hz}^{2/3}$. The single-octave SFDR at the third-order null bias is $132 \text{ dB} \cdot \text{Hz}^{4/5}$.

Index Terms—Electroabsorption modulator (EAM), peripheral coupled waveguide (PCW), radio-frequency (RF) link gain, spurious-free dynamic range (SFDR).

I. INTRODUCTION

FOR TRANSMISSION of radio-frequency (RF) signals in fibers, a popular choice is an externally modulated analog-optical link that consists of three principle parts. The transmitter consists of a laser followed by an optical modulator that impresses an RF signal onto the optical carrier. The modulated output is coupled to an optical fiber and detected by a photodetector, where it is demodulated back into an RF signal. One of the important figures of merit for any analog fiber-optic link is its conversion efficiency (or RF link gain), which for an externally modulated link is proportional to the square of the product of the optical power, the optical insertion loss, and the slope efficiency of the modulator [1]. A high RF gain (>30 dB) externally modulated link has been demonstrated at 150 MHz using a LiNbO₃ Mach-Zehnder modulator [2].

An electroabsorption modulator (EAM) is attractive due to its small size, high slope efficiency, large modulation bandwidth, and potential for monolithic integration with other optical and electrical components. There are several challenges in using a conventional EAM for RF link. In order to obtain both large modulation bandwidth and high slope efficiency, a traveling wave electrode is used to provide effective modulation over

extensive interaction length. However, the sharing of the electroabsorption (EA) layer in both the optical and the microwave waveguides results in a compromise of the EA layer thickness. The residual propagation loss due to scattering and the EA absorption at the bias voltage limit the device length to approximately 200–300 μm . The short length and the relative thick EA layer prevent us from getting very large slope efficiency (i.e., small equivalent half-wave voltage V_{π}). The high propagation loss also causes large optical insertion loss. The saturation effect of the photogenerated carriers limits the highest optical power handled by the device. All three factors (insertion loss, V_{π} , and optical saturation power) are limited in a conventional EAM, preventing us from getting high RF link gain.

By introducing the peripheral coupled waveguide (PCW) structure with respect to the EA layer [3], we decouple the microwave electrode and the optical designs in an EAM. The microwave electrode, including the EA region, is placed only peripheral to a large optical waveguide mode, in its evanescent field. The low confinement factor in the EA layer ($\sim 4.8\%$), in contrast to the conventional large optical cavity EAM design with typically large confinement factor ($>20\%$), reduces the photogenerated current per unit throughout power per unit length and, thus, enhances the optical power handling of the EAM. The design of the microwave electrode will affect minimally the optical mode, so one can use very small EA layer thickness to lower the V_{π} . As the guided optical mode is located away from the surface, it encounters a much smaller scattering loss. Thus, the insertion loss is reduced significantly. The device length can be increased to ensure a low V_{π} . The large optical waveguide mode will match better to the single-mode fiber mode.

The large optical waveguide mode has been used previously by other researchers primarily to achieve a better coupling to the single-mode optical fiber mode [4], [5], or to achieve better phase matching of microwave and optical phase velocities [6], or to reduce the photocurrent per unit length in detectors [7]. Only in the PCW design, it has been used primarily to reduce the photogenerated carrier per unit incident optical power and to decouple the microwave and optical waveguide designs. The reduction of scattering loss per unit length is also an important benefit.

To demonstrate this concept, a PCW EAM with lumped-electrode is reported in this letter, in which high optical saturation, low insertion loss, and low V_{π} all work together to give us an RF link gain of -3 dB with large spurious-free dynamic range

Manuscript received February 4, 2004; revised May 27, 2004. This work was supported in part by Defense Advanced Research Projects Agency (DARPA) RFLICS program, in part by Air Force Research Laboratory, and in part by National Science Foundation (NSF) ANIR.

The authors are with the Department of Electrical and Computer Engineering, Jacobs School of Engineering, University of California, San Diego, La Jolla, CA 92093 USA (e-mail: yzhuang@ucsd.edu; chang@ece.ucsd.edu; yu@ece.ucsd.edu).

Digital Object Identifier 10.1109/LPT.2004.833057

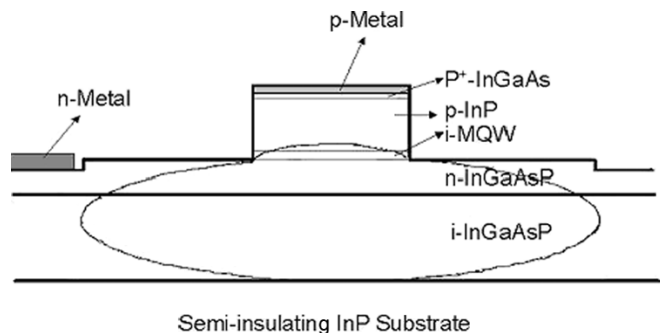


Fig. 1. Schematic cross section of a PCW EAM.

(SFDR). For a lumped-electrode device, the length of the electrode limits the electrical bandwidth because of its capacitance. A PCW EAM with traveling wave electrode design will not have this restriction [4]. It is under investigation and its performance will be reported later.

Prior to this work, we have demonstrated, using a combination of intrastep barrier quantum well (IQW) coupled with a single-side large optical waveguide, a high power operation of the EAM [5]. The confinement factor of the EA layer is still high (27%), leading to higher propagation loss and, thus, limits the waveguide length. The attainment of high saturation power in [5] is affected primarily by the IQW design.

II. DEVICE STRUCTURE AND FABRICATION

The p-i(MQW)-n waveguide modulator is grown on a semi-insulating InP substrate, as schematically shown in Fig. 1. The top InGaAs is 50 nm thick and is heavily doped ($1 \times 10^{19} \text{ cm}^{-3}$) for ohmic contact. The p-InP layer underneath is $0.75 \mu\text{m}$ thick ($5 \times 10^{17} \text{ cm}^{-3}$), followed by 70-nm-thick p-doped ($5 \times 10^{17} \text{ cm}^{-3}$) InGaAsP layer for fine tuning the confinement factor. The undoped multiple quantum-well (MQW) layer ($0.1 \mu\text{m}$ thick) consists of five periods of InGaAsP wells (10-nm-thick 0.80-eV bandgap) and InGaAsP barriers (7 nm thick; 1.08 eV bandgap). The exciton absorption peak of this MQW is at 1480 nm. InP-doping blocking layers (30 and 50 nm, respectively) are on the top and bottom of the MQWs, which are added to improve the breakdown voltage. Underneath the MQW layers is a $1.7\text{-}\mu\text{m}$ -thick InGaAsP (1.11 eV bandgap) lower cladding layer. The top portion, an n-InGaAsP ($3 \times 10^{18} \text{ cm}^{-3}$), is $0.6 \mu\text{m}$ thick with n-contact fabricated outside the wide ridge (see Fig. 1). The measured $1/e$ mode size is $11 \mu\text{m}$ by $3.5 \mu\text{m}$. The thickness of the InGaAsP has been limited, so far, by the growth process. The confinement factor of the EA layer is estimated to be $\sim 4.8\%$.

In Fig. 1, the two waveguide ridges are formed by chemical etching. The top one is $4 \mu\text{m}$ wide and includes the p- and i-regions. P-metal is evaporated on top of the ridge. The second ridge for the optical waveguide is formed by a shallow etching (about 200 nm) of the n-layer. The ridge is $12 \mu\text{m}$ wide to provide lateral optical modal confinement.

III. MODULATOR AND RF LINK PERFORMANCE

We tested a 1.3-mm-long lumped-element PCW-EAM, which has resistance-capacitance (RC)-limited 3-dB bandwidth of about 700 MHz. Fig. 2 shows its normalized transmission versus bias voltage at 1-, 10-, and 32-mW optical

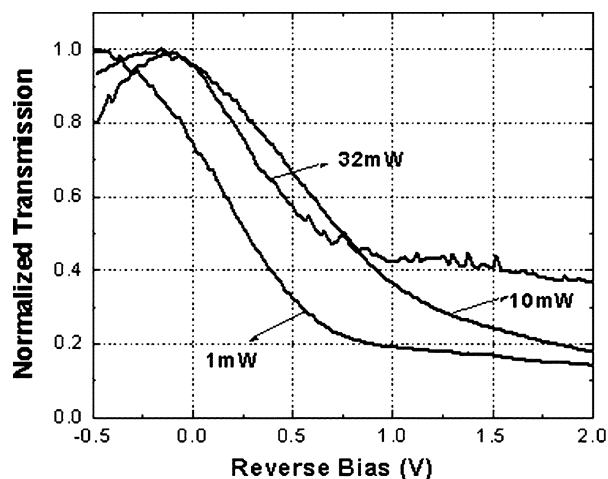


Fig. 2. Normalized transfer curve of the PCW-EAM at three different input optical powers.

input power. There is no antireflection coating deposited on the waveguide facets. The light source is a 1557-nm distributed feedback laser whose output is amplified by an erbium-doped fiber amplifier. The photodetector used has a responsivity of 0.8 A/W .

At 1-mW optical input, due to the built-in field, the smallest insertion loss occurs at 0.5-V forward bias. This uncoated modulator exhibits a fiber-to-fiber insertion loss of 10.6 dB at this bias which includes 1.5 dB of Fresnel loss at each facets, 1.45 dB of coupling losses to the lensed fibers (with $3\text{-}\mu\text{m}$ spot size) at each facet, and a propagation loss of $\sim 5 \text{ dB}$ ($\sim 4 \text{ dB/mm}$). The highest normalized slope efficiency of 1.2 V^{-1} was obtained from the transmission normalized to +0.5-V bias, which gives an equivalent V_{π} of 1.3 V. When the optical power is increased from 1 to 10 mW, the transfer curve shape changes. The highest transmission happens at about 0.1-V forward bias. The corresponding insertion loss at this bias is 10.2 dB; and the V_{π} is 1.8 V. When the optical power is increased to 32 mW, the insertion loss remains about the same, while the V_{π} is decreased to 1.6 V. There is insufficient data to determine the cause for the change of V_{π} . The change of the V_{π} may be caused by residual carrier screening effect and thermal-induced bandgap shrinkage. At 32 mW, it appears to have significant leakage of unmodulated optical power coupled to the output fiber at $V > 1$. The cause of this leakage is still under investigation. However, the slope efficiency of the device is not affected by this segment of the transmission curve for $V > 1$.

The RF link gain of an externally modulated optical link using this EAM has been measured at 500 MHz at different optical input power levels using the same components. The modulator is biased at the second-order null point. The RF link gain versus optical input power exhibits a slope of two in a log-log plot, as shown in Fig. 3. The highest link gain of -3 dB was obtained at 80-mW optical power, where the modulator still did not show any sign of saturation.

SFDR is another important link parameter. Nonlinearity of the link is often due to distortions generated at the modulator. In measuring the SFDRs of this device, the optical power is initially set at 80 mW (19 dBm). The two RF tones are at 490 and 510 MHz, respectively. For multioctave SFDR, the modulator is biased at the second-order null point (at -0.3 V bias), where

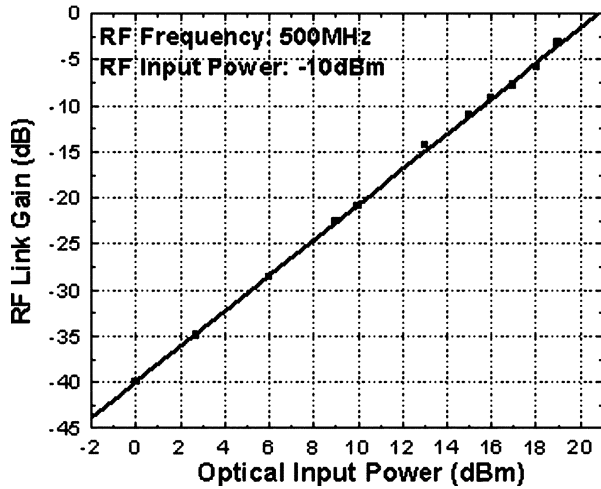


Fig. 3. RF link gain versus input optical power of the PCW-EAM.

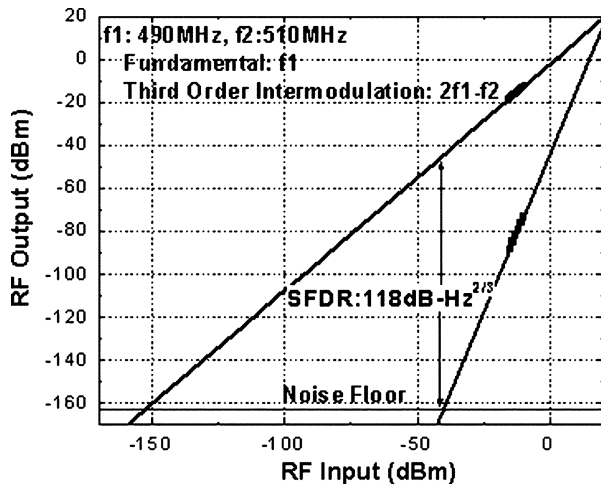


Fig. 4. Measured fundamental and third-order intermodulation distortion signals at the second-order null bias point.

the dc photocurrent at the detector is 3.1 mA. The shot noise at this photocurrent (−163 dBm) is the dominant noise of the link. Fig. 4 shows the fundamental output power and the output third-order intermodulation distortion (IM3) power versus input RF power in a log–log plot. The output fundamental signal has a slope of 1.05, and the IM3s is 2.96. From Fig. 4, we extracted a multioctave SFDR of $118 \text{ dB} \cdot \text{Hz}^{2/3}$.

For single-octave SFDR measurement, the modulator is biased at the third-order null point (reverse bias at 1.01 V). At this bias, the photocurrent at the detector is 1.4 mA. The corresponding noise floor is −166 dBm. Fig. 5 shows the fundamental output power and the IM3 spurious output power at this bias. The output fundamental signal has a slope of 0.92 and the IM3 has a slope of 5.03 (dominated by the fifth-order nonlinearity), giving a single-octave SFDR of $132 \text{ dB} \cdot \text{Hz}^{4/5}$.

At 1 GHz, the same EAM exhibits an RF link gain of −7 dB and a multioctave SFDR of $120 \text{ dB} \cdot \text{Hz}^{2/3}$, at the bias voltage of −0.3 V and at the input power of 63 mW. If we scale the input power to 80 mW, the link gain would be lower than that

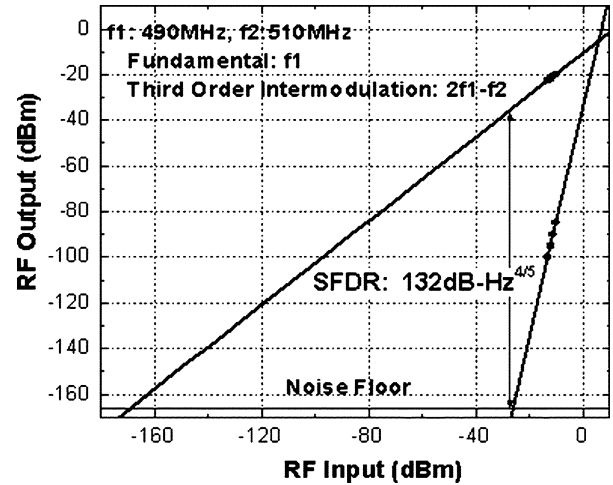


Fig. 5. Measured fundamental and third-order intermodulation distortion (fifth-order nonlinearity dominated) at the third-order null bias point.

measured at 510 MHz. The slight increase in SFDR is attributed to the reduction of IM3 at lower optical power.

IV. CONCLUSION

We have demonstrated a highly efficient PCW EAM for externally modulated analog fiber-optic link. The uncoated 1.3-mm-long lumped electrode EAM has a fiber-to-fiber insertion loss of 10.2 dB and an equivalent V_π of 1.3 V. An RF link gain of −3 dB is measured at 80-mW input optical power and at 500 MHz. The respective multioctave SFDR is $118 \text{ dB} \cdot \text{Hz}^{2/3}$ and the single-octave SFDR is $132 \text{ dB} \cdot \text{Hz}^{4/5}$. At 1 GHz, the RF link gain is −7 dB and the multioctave SFDR is $120 \text{ dB} \cdot \text{Hz}^{2/3}$.

For lumped electrode PCW EAM, the longer the electrode, the larger the electrode capacitance, the lower is the RC limited bandwidth. The bandwidth can be enhanced by using a traveling wave electrode in the design.

REFERENCES

- [1] C. Cox III, G. E. Betts, and L. M. Johnson, “An analytic and experimental comparison of direct and external modulation in analog fiber-optic links,” *IEEE Trans. Microwave Theory Tech.*, vol. 38, pp. 501–509, May 1990.
- [2] C. Cox III, E. Ackerman, and G. Betts, “Relationship between gain and noise figure of an optical analog link,” in *Dig. 1996 IEEE MTT-S Int. Microwave Symp.*, vol. 3, 1996, pp. 1551–1554.
- [3] P. K. L. Yu, W. S. C. Chang, Y. Zhuang, and G. L. Li, “Advances in traveling-wave electroabsorption modulators for analog applications,” in *Proc. LEOS 2001*, vol. 2, 2001, pp. 540–541.
- [4] G. L. Li, S. A. Pappert, P. Mages, C. K. Sun, W. S. C. Chang, and P. K. L. Yu, “High-saturation high-speed traveling-wave InGaAsP-InP electroabsorption modulator,” *IEEE Photon. Technol. Lett.*, vol. 13, pp. 1076–1078, Oct. 2001.
- [5] J. X. Chen, Y. Wu, W. X. Chen, I. Shubin, A. Clawson, W. S. C. Chang, and P. K. L. Yu, “High-power intrastep quantum well electroabsorption modulator using single-sided large optical cavity waveguide,” *IEEE Photon. Technol. Lett.*, vol. 16, pp. 440–442, Feb. 2004.
- [6] Y. T. Byun, K. H. Park, S. H. Kim, S. S. Choi, J. C. Yi, and T. K. Lim, “Efficient single-mode GaAs/AlGaAs waveguide phase modulator with a low propagation loss,” *Appl. Opt.*, vol. 37, pp. 496–501, 1998.
- [7] M. S. Islam, T. Jung, S. Murthy, T. Itoh, M. C. Wu, D. L. Sivco, and A. Y. Cho, “Velocity-matched distributed photodetectors with p-i-n photodiodes,” in *Dig. Int. Topical Meeting Microwave Photonics*, 2000, pp. 217–220.